

Parsing Squeezed Light into Polarization Manifolds

C. R. Müller,^{1,2,3} L. S. Madsen,³ A. Klimov,⁴ L. L. Sánchez-Soto,^{5,1,2} G. Leuchs,^{1,2} Ch. Marquardt,^{1,2,3} and U. L. Andersen^{3,1}

¹Max-Planck-Institut für die Physik des Lichts, Günther-Scharowsky-Straße 1, Bau 24, 91058 Erlangen, Germany

²Institut für Optik, Information und Photonik, Universität Erlangen-Nürnberg, Staudtstraße 7/B2, 91058 Erlangen, Germany

³Department of Physics, Technical University of Denmark, Fysikvej, 2800 Kgs. Lyngby, Denmark

⁴Departamento de Física, Universidad de Guadalajara, 44420 Guadalajara, Jalisco, Mexico

⁵Departamento de Óptica, Facultad de Física, Universidad Complutense, 28040 Madrid, Spain

We investigate polarization squeezing in squeezed coherent states with varying coherent amplitudes. In contrast to the traditional characterization based on the full Stokes parameters, we experimentally determine the Stokes vector of each excitation manifold separately. Only for states with a fixed photon number do the methods coincide; when the photon number is indefinite, our approach gives a richer and deeper description. By capitalizing on the properties of the Husimi Q function, we map this notion onto the Poincaré space, providing a full account of the measured squeezing.

PACS numbers: 42.50.Dv, 42.50.Lc, 03.65.Wj

Heisenberg's uncertainty principle [1] epitomizes the basic tenets of quantum theory and it comes out as a strict trade-off: fluctuations of a given observable can always be reduced below some threshold at the expense of an increase in the fluctuations of another observable. A time-honored example of this trade-off is provided by quadrature squeezed states of light [2], which can be generated, for example, with lower uncertainty in their amplitude and higher uncertainty in their phase.

The notion of squeezing, while universal for harmonic oscillator-like systems, is otherwise far from unique. For spin-like systems there are several approaches [3–5]: all of them compare fluctuations of suitably chosen observables with a threshold given by some reference state. Spin squeezed states have attracted a lot of attention in recent years as they might constitute an important resource in quantum information [6, 7].

As the Stokes operators [8], specifying the polarization properties of quantum fields, match the standard features of an angular momentum, the parallel between spin and polarization squeezing [9] cannot come as a surprise. Actually, for states with fixed photon number both notions coincide and have been experimentally demonstrated [10]. In the opposite regime of an indefinite number of photons (often involving bright states [11]), polarization squeezing has been reported in numerous systems, including parametric amplifiers [12, 13], optical fibers [14, 15], and atomic vapors [16, 17]. The uncertainty in photon number now forces us to scrutinize multiple excitation manifolds.

Until now there have been no studies on the transition between these two regimes. The goal of this Letter is to explore both within a single experiment. Using two optical parametric amplifiers, complemented with a phase-space displacement, we squeeze various fixed photon-number manifolds. Polarization squeezing is analyzed as a function of the coherent amplitude, finding out that this operation tends to degrade squeezing. Besides, this transition from vacuum squeezing to displaced vacuum squeezing can be clearly visualized in Poincaré space using the appropriate Husimi Q representation.

Let us start by briefly recalling some basic notions. We shall be dealing with monochromatic fields, defined by two operators \hat{a}_H and \hat{a}_V : they represent the complex amplitudes in two linearly polarized orthogonal modes, that we indicate as horizontal (H) and vertical (V), respectively. The Stokes operators are [18]

$$\begin{aligned}\hat{S}_x &= \frac{1}{2}(\hat{a}_H^\dagger \hat{a}_V + \hat{a}_V^\dagger \hat{a}_H), & \hat{S}_y &= \frac{i}{2}(\hat{a}_H \hat{a}_V^\dagger - \hat{a}_H^\dagger \hat{a}_V), \\ \hat{S}_z &= \frac{1}{2}(\hat{a}_H^\dagger \hat{a}_H - \hat{a}_V^\dagger \hat{a}_V),\end{aligned}\quad (1)$$

together with the total photon number $\hat{N} = \hat{a}_H^\dagger \hat{a}_H + \hat{a}_V^\dagger \hat{a}_V$. The components of the vector $\hat{\mathbf{S}} = (\hat{S}_x, \hat{S}_y, \hat{S}_z)$ thus satisfy the commutation relations of the $\mathfrak{su}(2)$ algebra: $[\hat{S}_x, \hat{S}_y] = i\hat{S}_z$ and cyclic permutations (we use $\hbar = 1$ throughout).

In classical optics, we have a Poincaré sphere with radius equal to the intensity, which is a sharp quantity. In contradistinction, in quantum optics Eq. (1) implies that $\hat{\mathbf{S}}^2 = \hat{S}_x^2 + \hat{S}_y^2 + \hat{S}_z^2 = S(S+1)\hat{\mathbb{I}}$, with $S = N/2$ playing the role of the spin. When the photon number is fuzzy, we need to consider a three-dimensional Poincaré space (with axis S_x , S_y , and S_z). This space can be visualized as a set of nested spheres with radii proportional to the diverse photon numbers that contribute to the state and that can be aptly called the polarization manifolds.

Since $[\hat{N}, \hat{\mathbf{S}}] = 0$, each excitation manifold should be addressed independently. This can be underlined if instead of the Fock basis $\{|n_H, n_V\rangle\}$, we employ the relabeling $|S, m\rangle \equiv |n_H = S + m, n_V = S - m\rangle$ that can be seen as the common eigenstates of \hat{S}^2 and \hat{S}_z . Note that $S = (n_H + n_V)/2$ and $m = (n_H - n_V)/2$. Moreover, the moments of any energy-preserving observable $f(\hat{\mathbf{S}})$ do not depend on the coherences between manifolds or on global phases: the only accessible polarization information from any density matrix $\hat{\rho}$ (which describes the state) is in its block-diagonal form $\hat{\rho}_{\text{pol}} = \oplus_S \hat{\rho}^{(S)}$, where $\hat{\rho}^{(S)}$ is the reduced density matrix in the subspace with spin S . Accordingly, we drop henceforth the subscript pol. This $\hat{\rho}_{\text{pol}}$ has been dubbed the polarization sector [19] or the polarization density matrix [20].

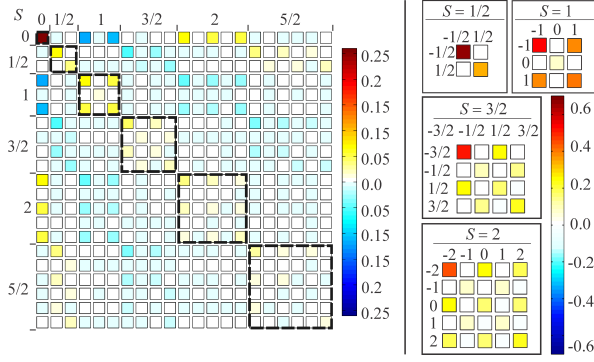


FIG. 1. (color online) Illustration of the measured polarization sector (black blocks) for a polarization squeezed state as in Eq. (3), with $\alpha = 1.13$. The subplots at the right depict different individually-normalized manifolds.

An example of the density matrix of one of our experimentally acquired states is shown in Fig. 1, where the sub-matrices associated with different polarization manifolds are displayed.

The shot-noise limit in the manifold of spin S (i.e., $N = 2S$ photons) is settled in terms of $SU(2)$ (or spin) coherent states [21]. They are defined as $|S, \mathbf{n}\rangle = \hat{D}(\mathbf{n})|S, S\rangle$, where \mathbf{n} is a unit vector [with spherical angles (θ, ϕ)] on the Poincaré sphere of radius $\sqrt{S(S+1)}$ and $\hat{D}(\mathbf{n}) = e^{i\theta\hat{S}_y}e^{i\phi\hat{S}_z}$ plays the role of a displacement on that sphere. For these states the variances of the Stokes operators $[\Delta^2\hat{S}_k = \langle\hat{S}_k^2\rangle - \langle\hat{S}_k\rangle^2]$ depend on \mathbf{n} , and there exists a preferred direction: the mean-spin direction. The corresponding variances in the direction \mathbf{n}_\perp perpendicular to the mean spin are isotropic and $\Delta^2\hat{S}_{\mathbf{n}_\perp} = S/2$, which is taken as the shot noise. In consequence, polarization squeezing for an arbitrary state occurs whenever the condition $\inf_{\mathbf{n}} \Delta^2\hat{S}_{\mathbf{n}} < S/2$ holds true.

A way to get around the dependence on the directions is to use the real symmetric 3×3 covariance matrix for the Stokes variables [22], defined as $\Gamma_{k\ell} = \frac{1}{2}\langle\{\hat{S}_k, \hat{S}_\ell\}\rangle - \langle\hat{S}_k\rangle\langle\hat{S}_\ell\rangle$, where $\{\cdot, \cdot\}$ is the anticommutator. In terms of this matrix Γ , we have $\Delta^2\hat{S}_{\mathbf{n}} = \mathbf{n}^t \Gamma \mathbf{n}$ and, since Γ is positive definite, the minimum of $\Delta^2\hat{S}_{\mathbf{n}}$ exists and it is unique. If we incorporate the constraint $\mathbf{n}^t \cdot \mathbf{n} = 1$ as a Lagrange multiplier γ , this minimum is given by $\Gamma \mathbf{n} = \gamma \mathbf{n}$: the admissible values of γ are thus the eigenvalues of Γ and the directions minimizing $\Delta^2\hat{S}_{\mathbf{n}}$ are the corresponding eigenvectors. Therefore, we can define the degree of polarization squeezing as

$$\xi^2 = \inf_{\mathbf{n}} \frac{\Delta^2\hat{S}_{\mathbf{n}}}{S/2} = \frac{4\gamma_{\min}}{N}. \quad (2)$$

We stress, though, that this definition is not unique and a number of proposals can be found in the literature, each one being specially tailored for specific purposes [5].

When the state spans several manifolds, we follow Ref. [23] and bring to bear an averaged Stokes vector $\langle\hat{\mathbf{S}}\rangle = \sum_{S=0}^{\infty} P_S \text{Tr}(\hat{\rho}^{(S)}\hat{\mathbf{S}})$, where P_S is the photon-number distribution. As a result, the squeezing of the state can be much lower than the corresponding one in the individual manifolds.

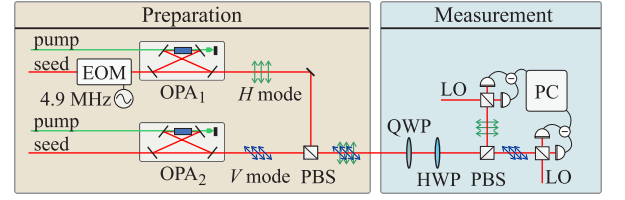


FIG. 2. (color online) Experimental setup. Two optical parametric amplifiers (OPA1 and OPA2) independently squeeze coherent seed beams in orthogonal polarization modes H and V . The seed beam entering OPA1 is modulated at the sideband frequency of 4.9 MHz. The modes are spatially combined on a polarizing beam splitter (PBS) and interference between the modes can be adjusted with the combination of a quarter wave-plate (QWP) and a half wave-plate (HWP). The polarization states are separated into orthogonal components followed by homodyne tomography.

To confirm these issues we use the setup sketched in Fig. 2. It comprises two optical parametric amplifiers (OPA1 and OPA2) operating below threshold and pumped with a 532 nm continuous-wave laser beam to produce two quadrature squeezed states. The parametric down-conversion processes are based on type I quasi-phase-matched periodically poled KTP crystals and generate squeezed states in one polarization mode. The OPAs were seeded with dim laser beams at 1064 nm to facilitate the locking (Pound-Drever-Hall technique [24]) of the cavities and several phases of the experiment. One of the seed beams is modulated via an electro-optical modulator (EOM) at the sideband frequency of 4.9 MHz relative to the carrier frequency and with variable modulation depth, allowing to control the amplitude of the thereby generated coherent states. The resulting modes are combined on a polarizing beam splitter (PBS) to form the state

$$|\Psi\rangle = \hat{S}(r_H)\hat{D}(\alpha_H)|0_H\rangle \otimes \hat{S}(r_V)|0_V\rangle. \quad (3)$$

Here, $\hat{D}(\alpha) = \exp(\alpha\hat{a}^\dagger - \alpha^*\hat{a})$ is the displacement and $\hat{S}(r) = \exp[(r^*\hat{a}^2 - r\hat{a}^{\dagger 2})/2]$ is the squeezing operator. The indexes H and V denote the mode to which the operator is applied. Since $r_H \simeq r_V \simeq 0.41$, we drop the corresponding subscripts. In addition, α will subsequently designate the amplitude of the horizontal component of the state after OPA1, which has been constrained to be a real number. Experimentally, we achieve about 3.6 dB of quadrature squeezing in both modes and about 4.4 dB of excess noise along the anti-squeezing direction.

To characterize the polarization state, the beam is directed to the verification stage. A quarter wave-plate (QWP) and a half-wave plate (HWP) allow to verify the interference between the orthogonal polarization modes and to control the measurement basis. To ease the otherwise complicated two-mode tomography, the original horizontal and vertical polarization modes are separated by a PBS and each one is characterized via homodyne tomography. The measurement is performed at the sideband frequency of 4.9 MHz with a bandwidth of 90 kHz. The local oscillator (LO) phases are scanned continuously to acquire the tomographic data and the homo-

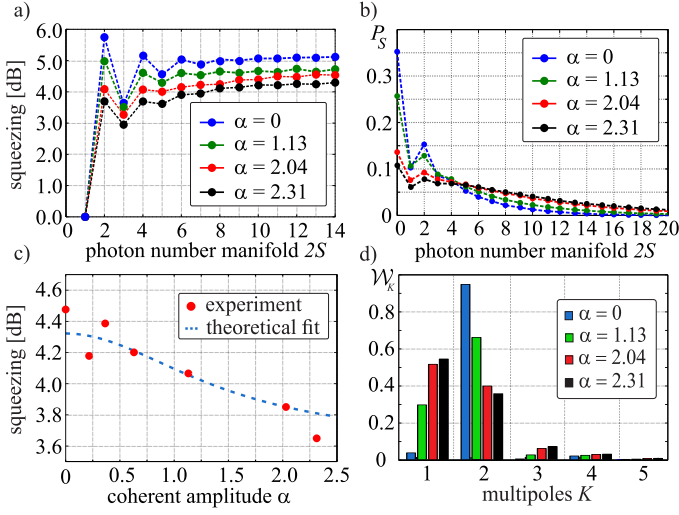


FIG. 3. (color online) Experimental results for different values of the coherent amplitude α . (a) Polarization squeezing as a function of the excitation manifold. (b) Photon-number distributions. (c) Polarization squeezing of the total state as a function of the coherent amplitude α . (d) Distribution of \mathcal{W}_K as a function of the multipole order K .

dyne outputs are stored in a computer. We determine the phase of the LO scans in the data, which allows one to compensate for any phase drifts among the two measurement stages in the post processing steps. The same data are then analyzed for noise properties at the measurement frequency.

In Fig. 3(a) we plot the measured polarization squeezing in the different excitation manifolds for various values of the coherent amplitude α . Squeezing occurs for all photon numbers except for the vacuum and the one-photon manifolds. This is intuitively clear, for squeezing the Stokes variables involves nonclassical correlations among individual photons: such correlations thus require the presence of at least two photons. For $S = 1$, these correlations are dramatically demonstrated by the presence of 6 dB polarization squeezing (for $\alpha = 0$).

Polarization squeezing is not equally distributed among the manifolds, but exhibits an oscillating pattern that is most pronounced for small S and small amplitude states. If the individual modes were ideally squeezed vacua ($\alpha = 0$) and were measured with perfect detectors, only even-photon number manifolds would contribute. Due to the additional excess noise of about 4.4 dB and the finite efficiency of the homodyne detectors (98% quantum efficiency of the photo diodes, $85 \pm 5\%$ total efficiency), however, the photon-number contributions are smeared out, as corroborated by Fig. 3(b), and polarization squeezing can also be observed for odd-excitation manifolds.

Increasing α results in an overall reduction of the polarization squeezing. The coherent amplitude acts much the same as a local oscillator, in such a way that the spin squeezing is continuously transferred into a quadrature measurement [25]. This coincides with the direct measurement of the bright squeezed vacuum states in Ref. [26]

The polarization squeezing of the entire state is also presented in Fig. 3(c) as a function of α . The experimental results are compared to a numerical simulation based on the measured single-mode squeezing and excess noise. For small amplitudes, mainly the inner manifolds dominate the squeezing. In the opposite limit of large amplitudes, the Stokes measurement reduces to a quadrature measurement, and thus the degree of polarization squeezing will no longer be determined by the photon-number correlations but by quadrature correlations. Deviations from the theoretical curve are due to small fluctuations in the squeezing and excess noise parameters between individual measurement runs.

It is worth stressing that parsing the state into manifolds turns out to be crucial to analyze the experimental results. If one computes the covariance matrix of Eq. (3) deemed as a two-mode state, one gets, after some calculations,

$$\xi^2 = \frac{4\gamma_{\min}}{\langle \hat{N} \rangle} \simeq \frac{|\alpha|^2 e^{-r}}{|\alpha|^2 + \frac{1}{2} \sinh^2 r}, \quad (4)$$

where a direct extension of Eq. (2) has been used. Whereas this gives the correct limit discussed before for $\alpha \rightarrow \infty$, it fails to reproduce the observed squeezing for $\alpha \rightarrow 0$.

We also lay out a phase-space picture of our previous discussion. A very handy way to convey the full information of the density matrix $\rho^{(S)}$ associated to our states in Eq. (3) is through the Husimi Q function, defined as $Q^{(S)}(\mathbf{n}) = \langle S, \mathbf{n} | \hat{\rho}^{(S)} | S, \mathbf{n} \rangle$. In this way, $Q^{(S)}(\mathbf{n})$ appears as the projection onto SU(2) coherent states, which have the most definite polarization allowed by quantum theory. When the state involves multiple manifolds we have

$$Q(\mathbf{n}) = \sum_S \frac{2S+1}{4\pi} Q^{(S)}(\mathbf{n}). \quad (5)$$

This is an appealing feature of this function: because of the lack of the off-diagonal contributions with $S \neq S'$, the Q function takes the form of an average over the manifolds with definite total number of excitations. Actually, the sum over S in Eq. (5) removes the total intensity of the field in such a way that $Q(\mathbf{n})$ contains only the relevant polarization information.

The expansion coefficients of $Q^{(S)}(\mathbf{n})$ in spherical harmonics, which are a basis for the functions on the sphere \mathcal{S}^2 , read

$$\rho_{Kq}^{(S)} = \sqrt{\frac{2S+1}{4\pi}} \frac{1}{C_{SS,K0}^{SS}} \int_{\mathcal{S}^2} d^2\mathbf{n} Y_{Kq}(\mathbf{n}) Q^{(S)}(\mathbf{n}), \quad (6)$$

where $K = 0, \dots, 2S$ and $C_{SS,K0}^{SS}$ is a Clebsch-Gordan coefficient introduced for a proper normalization. The $\rho_{Kq}^{(S)}$ are the standard state multipoles [27], proportional to the K th power of the Stokes variables. They can also be related to measures of state localization on the sphere [28].

The quantity $\mathcal{W}_K^{(S)} = \sum_{q=-K}^K |\rho_{Kq}^{(S)}|^2$ is the square of the state overlapping with the K th multipole pattern in the S th subspace. When there is a distribution of photon numbers, we sum over all of them to obtain \mathcal{W}_K [29]. In Fig. 3(d) we represent \mathcal{W}_K as a function of the multipole order for four values of the amplitude α . From a practical viewpoint only the

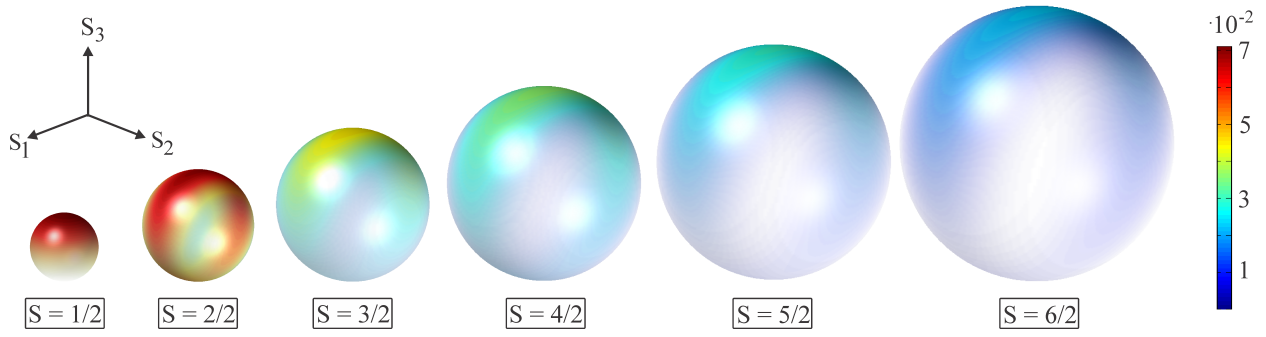


FIG. 4. (color online) Reconstructed $SU(2)$ $Q^{(S)}$ functions of the excitation manifolds indicated in the insets for a polarization squeezed state with $\alpha = 1.13$. The scale of the density plots on the corresponding Poincaré spheres is shown on the right.

dipole ($K = 1$) and the quadrupole ($K = 2$) are noticeable. For $\alpha = 0$ the dipole is almost negligible while the quadrupole is the leading contribution. The dipole becomes larger as α increases, whereas the opposite happens for the quadrupole: a clear indication that the state gets more and more localized.

In Fig. 4 we plot the Husimi function of the first six manifolds of a squeezed coherent state as in Eq. (3), with $\alpha = 1.13$. The birth of polarization squeezing is nicely observed: for the one-photon manifold, the polarization spreads over the sphere and we expect no squeezing, whereas in the two-photon manifold the uncertainty becomes squeezed and belts around the sphere. As the photon number is further increased, the squeezing becomes more evident and the uncertainty area becomes more localized, tracing out a squeezed ellipse on the sphere.

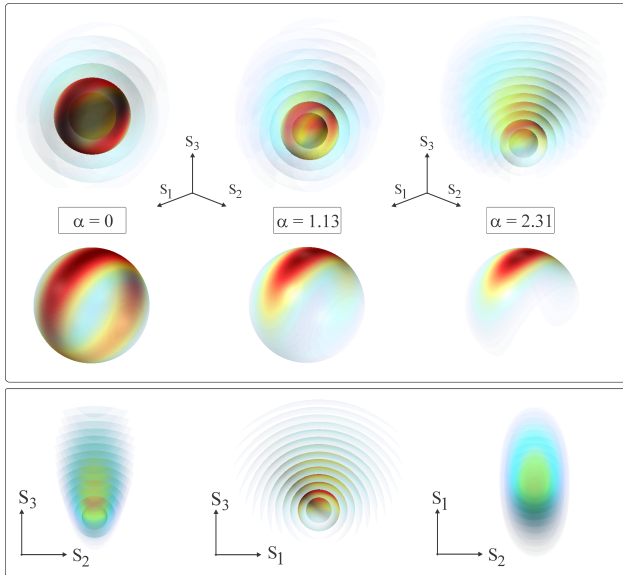


FIG. 5. (color online) Top panel: Reconstructed $SU(2)$ Husimi functions of the polarization squeezed states for three different coherent amplitudes $\alpha = 0, 1.13$, and 2.31 , from left to right. In the upper row, we represent the parsed version, foliated into suitably scaled polarization manifolds in Poincaré space. In the lower row, we have the total Q function as given by Eq. (5). Bottom panel: Views along the coordinate axes of the state with $\alpha = 2.31$.

In Fig. 5 the Husimi function of the entire state parsed in its manifolds is illustrated for three displacements. When $\alpha = 0$, the innermost sphere with $S = 1/2$ is highly occupied, while the outer ones are almost empty. A strong directional bias appears when α increases. We also plot the total Q computed as in Eq. (5), wherein the squeezing becomes conspicuous. In the bottom panel we include the views of the parsed Husimi function along the three coordinate axes for the state with $\alpha = 2.31$. The typical cigar-like projections, familiar from previous measurements [26], can be recognized.

In summary, we have presented a complete characterization of polarization squeezing of squeezed coherent states. Parsing the Poincaré space into excitation manifolds has played a pivotal role. By varying the coherent amplitude, we have witnessed the transition from states living in one single manifold to those spreading over many of them. Far from being an academic curiosity, this has allowed us to clarify previous discrepancies with the experiment. Using the Husimi Q function for the problem at hand we have been able to envision that transition in a very intuitive manner.

Financial support from the Lundbeck foundation, the Danish Council for Independent Research (Sapere Aude 0602-01686B), the European Union FP7 (Grant QESSENCE), the European Research Council (Advanced Grant PACART), the Mexican CONACyT (Grant 254127), and the Program UCM-BSCH (Grant GR3/14) is gratefully acknowledged.

-
- [1] P. Busch, T. Heinonen, and P. Lahti, “Heisenberg’s uncertainty principle,” *Phys. Rep.* **452**, 155–176 (2007).
 - [2] A. I. Lvovsky, “Fundamentals of Photonics and Physics,” (Wiley, Hoboken, NJ, 2015) Chap. Squeezed Light, pp. 121–164.
 - [3] M. Kitagawa and M. Ueda, “Squeezed spin states,” *Phys. Rev. A* **47**, 5138–5143 (1993).
 - [4] W. M. Itano, J. C. Bergquist, J. J. Bollinger, J. M. Gilligan, D. J. Heinzen, F. L. Moore, M. G. Raizen, and D. J. Wineland, “Quantum projection noise: Population fluctuations in two-level systems,” *Phys. Rev. A* **47**, 3554–3570 (1993).
 - [5] J. Ma, X. Wang, C.P. Sun, and F. Nori, “Quantum spin squeezing,” *Phys. Rep.* **509**, 89–165 (2011).
 - [6] C. Gross, “Spin squeezing, entanglement and quantum metrol-

- ogy with Bose–Einstein condensates,” *J. Phys. B* **45**, 103001 (2012).
- [7] O. Gühne and G. Tóth, “Entanglement detection,” *Phys. Rep.* **474**, 1–75 (2009).
- [8] J. M. Jauch and F. Rohrlich, *Theory of Photons and Electrons* (Addison-Wesley, New York, 1955).
- [9] A. S. Chirkin, A. A. Orlov, and D. Yu. Parashchuk, “Quantum theory of two-mode interactions in optically anisotropic media with cubic nonlinearities: Generation of quadrature- and polarization-squeezed light,” *Quantum Electron.* **23**, 870–874 (1993).
- [10] L. K. Shalm, R. B. A. Adamson, and A. M. Steinberg, “Squeezing and over-squeezing of triphotons,” *Nature* **457**, 67–70 (2009).
- [11] N. Korolkova, G. Leuchs, R. Loudon, T. C. Ralph, and C. Silberhorn, “Polarization squeezing and continuous-variable polarization entanglement,” *Phys. Rev. A* **65**, 052306 (2002).
- [12] M. Lassen, M. Sabuncu, P. Buchhave, and U. L. Andersen, “Generation of polarization squeezing with periodically poled KTP at 1064 nm,” *Opt. Express* **15**, 5077 (2007).
- [13] T. S. Iskhakov, M. V. Chekhova, and G. Leuchs, “Generation and direct detection of broadband mesoscopic polarization-squeezed vacuum,” *Phys. Rev. Lett.* **102**, 183602 (2009).
- [14] J. Heersink, V. Josse, G. Leuchs, and U. L. Andersen, “Efficient polarization squeezing in optical fibers,” *Opt. Lett.* **30**, 1192–1194 (2005).
- [15] Ch. Marquardt, J. Heersink, R. Dong, M. V. Chekhova, A. B. Klimov, L. L. Sánchez-Soto, U. L. Andersen, and G. Leuchs, “Quantum reconstruction of an intense polarization squeezed optical state,” *Phys. Rev. Lett.* **99**, 220401 (2007).
- [16] V. Josse, A. Dantan, L. Vernac, A. Bramati, M. Pinard, and E. Giacobino, “Polarization squeezing with cold atoms,” *Phys. Rev. Lett.* **91**, 103601 (2003).
- [17] S. Barreiro, P. Valente, H. Failache, and A. Lezama, “Polarization squeezing of light by single passage through an atomic vapor,” *Phys. Rev. A* **84**, 033851 (2011).
- [18] A. Luis and L. L. Sánchez-Soto, “Quantum phase difference, phase measurements and Stokes operators,” *Prog. Opt.* **41**, 421–481 (2000).
- [19] M. G. Raymer, D. F. McAlister, and A. Funk, “Measuring the quantum polarization state of light,” in *Quantum Communication, Computing, and Measurement 2*, edited by P. Kumar (Plenum, New York, 2000).
- [20] V. P. Karassiov and A. V. Masalov, “The method of polarization tomography of radiation in quantum optics,” *JETP* **99**, 51–60 (2004).
- [21] A. Perelomov, *Generalized Coherent States and their Applications* (Springer, Berlin, 1986).
- [22] A. B. Klimov, G. Björk, J. Söderholm, L. S. Madsen, M. Lassen, U. L. Andersen, J. Heersink, R. Dong, Ch. Marquardt, G. Leuchs, and L. L. Sánchez-Soto, “Assessing the polarization of a quantum field from Stokes fluctuations,” *Phys. Rev. Lett.* **105**, 153602 (2010).
- [23] C. Kothe, L. S. Madsen, U. L. Andersen, and G. Björk, “Experimental determination of the degree of polarization of quantum states,” *Phys. Rev. A* **87**, 043814 (2013).
- [24] R. W. P. Drever, J. L. Hall, F. V. Kowalski, J. Hough, G. M. Ford, A. J. Munley, and H. Ward, “Laser phase and frequency stabilization using an optical resonator,” *Appl. Phys. B* **31**, 97–105 (1983).
- [25] X. Wang and B. C. Sanders, “Relations between bosonic quadrature squeezing and atomic spin squeezing,” *Phys. Rev. A* **68**, 033821 (2003).
- [26] C. R. Müller, B. Stoklasa, C. Peuntinger, C. Gabriel, J. Řeháček, Z. Hradil, A. B. Klimov, G. Leuchs, C. Marquardt, and L. L. Sánchez-Soto, “Quantum polarization tomography of bright squeezed light,” *New J. Phys.* **14**, 085002 (2012).
- [27] K. Blum, *Density Matrix Theory and Applications* (Plenum, New York, 1981).
- [28] L. L. Sánchez-Soto, A. B. Klimov, P. de la Hoz, and G. Leuchs, “Quantum versus classical polarization states: when multipoles count,” *J. Phys. B* **46**, 104011 (2013).
- [29] P. de la Hoz, A. B. Klimov, G. Björk, Y. H. Kim, C. Müller, Ch. Marquardt, G. Leuchs, and L. L. Sánchez-Soto, “Multipolar hierarchy of efficient quantum polarization measures,” *Phys. Rev. A* **88**, 063803 (2013).